

Design And Analysis Of An Open Differential

Subhajit Konar^{1,*}, Vijay Gautam²

(^{1,2}Delhi Technological University, Delhi 110042)

Email: subhokonar94@gmail.com

<https://doi.org/10.35121/ijapie201904232>

Abstract : An automobile differential gear system is used to establish a differential motion between left and right driving axle which provides a smooth turning of the vehicle. When a vehicle takes a turn then the wheels at outermost position requires to cover a large distance than that of the innermost wheels. This speed variation can be achieved by using a differential gear system. It also transmits the power from the propeller shaft to each axle. A rear wheel drive vehicle requires a differential at the rear axle while all-wheel drive vehicle requires differential gear system for each and every axle. In this paper, an open differential is designed for a leading automobile and analysed the ability to work without failure. The analysis was done using the modified Lewis equation, Hertzian contact stress equation and AGMA equations. The analytical results were compared with results obtained by FEA. It is observed that results obtained from Lewis criterion are more conservative as compared to AGMA. The results obtained from modified Lewis, Hertzian contact stress and AGMA are in good agreement with the results obtained from FEA.

Keywords: Differential, axle, AGMA equations, Hertz contact stress, FEA.

1. INTRODUCTION

A differential is a device that splits the engine torque and supplies to the outer wheels, allowing each outer wheel to rotate at different speed [1]. The differential is found on all modern cars and trucks. In automobiles and other wheeled vehicles, the differential allows the outer drive wheel to rotate faster than the inner drive wheel during a turn. This is necessary when the vehicle turns, making the wheel that is traveling around the outside of the turning curve roll farther and faster than the other. The average of the rotational speed of the two driving wheels equals the input rotational speed of the drive shaft. An increase in the speed of one wheel is balanced by a decrease in the speed of the other. differential has mainly 3 functions- (1) It directs power from the engine to the wheels (2) It acts as the final gear reduction in vehicle (3) The differential transmits power to different wheels while allowing them to rotate at different speeds [2].

2. WORKING PRINCIPLE OF DIFFERENTIALS

When an automobile travels around a corner, the distance travelled by the outside wheels is greater than that travelled by the inside wheels. If the wheels are mounted on dead axles so that they turn independently of each other, like the front wheels of an ordinary passenger vehicle, they will turn at different speeds to compensate for the difference in travel. But, if the wheels are driven positively by the engine, a device is necessary which will permit them to revolve at different speeds without interfering with the propulsion

system. To accomplish this purpose a system of gears called the differential is provided.

The driving axle is one of the cross members which supports the load of the tractor, and has the driving wheels at its ends. The driving axle consists of a housing, a differential, two axle shafts (half axles), and final drives (if required).

The differential is an important component of the driving axle. The main functions performed by the differential system are:

- Further reduces the rotations coming from the gear box before the same are passed on to the rear axles.
- Changes the direction of axis of rotation of the power by 90° i.e. from being longitudinal to transverse direction.
- To distribute power equally to both the rear driving axles when the tractor is moving in straight ahead direction.
- To distribute the power as per requirement to the driving axles during turning i.e. more rotations are required by the outer wheel as compared to the inner wheel – during turns.
- To increase the tractive effort as per requirement, all wheel drive and four-wheel drive systems plays an important role to avoid loss of traction force while the vehicle is in action

3.

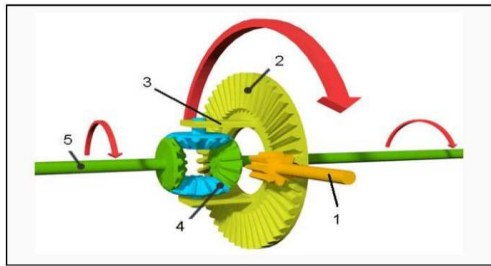


Fig. 1: Construction of a differential gear mechanism [3]

The main components of the differential as shown in Fig.1 are:

- Input pinion gear-1
- Crown wheel gear-2
- Differential cage-3
- Differential star-4
- Differential axle (sun) gear-5

3. DIFFERENT TYPES OF DIFFERENTIAL GEAR MECHANISM

A. Locked differential

A locking differential locks the rotational speed of the axle shafts, forcing the left and right wheels to turn at the same rate [4]. This happens regardless of which axle has traction or is losing traction. A locking differential is designed to overcome the chief limitation of a standard open differential by essentially "locking" both wheels on an axle together as if on a common shaft [4]. This force both wheels to turn in unison, regardless of the traction available to either wheel individually. When the differential is unlocked (open differential), it allows each wheel to rotate at different speeds (such as when negotiating a turn). An open (or unlocked) differential always provides the same torque (rotational force) to each of the two wheels, on that axle. So, although the wheels can rotate at different speeds, they apply the same rotational force, even if one is entirely stationary, and the other spinning. (Equal torque, unequal rotational speed). By contrast, a locked differential force both left and right wheels on the same axle to rotate at the same speed under nearly all circumstances, without regard to traction differences seen at either wheel. Therefore, each wheel can apply as much rotational force as the traction under it will allow, and the torques on each side-shaft will be unequal.

B. Limited slip differential

Limited slip differentials are made to limit the tendency of an open differential to send power to a wheel that's losing traction. Limited slip sends power to both wheels at the same rate when travelling straight. If one wheel loses traction and begins faster, the differential will automatically direct torque to the other wheel. Essentially, limited slip or

differentials send power from the wheel that's slipping to the wheel that isn't. Limited-slip style differentials can function using any number of mechanisms: clutches, gears, viscous coupling, etc. Limited slip differentials are good for daily driven vehicles as well as 4x4 vehicles.

Fourier-Transform Infrared Spectroscopy (FTIR)

Fig. 1 shows the IR spectra for untreated and alkali treated pineapple leaf fiber (PALF) that was obtained by using the FTIR spectrometer.

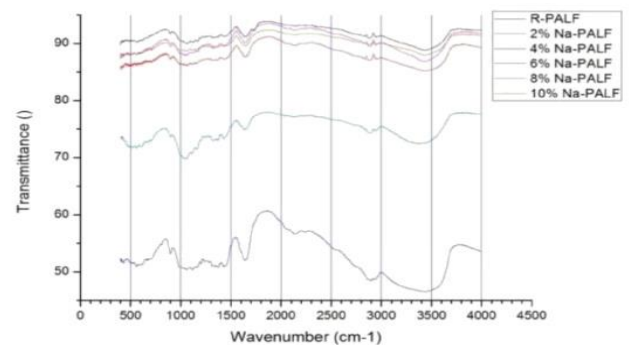


Fig. 1: IR spectra of untreated and alkali treated pineapple leaf fibers

The broad peak between 3200 cm^{-1} to 3500 cm^{-1} is linked to OH stretching vibration present in amorphous and crystalline cellulose. The carbonyl stretching ($\text{C}=\text{O}$) peak (1730 cm^{-1}) related to hemicellulose can be seen in untreated PALF but not present in alkali treated pineapple leaf fibers. This may be due to the removal of hemicellulose component. CH_2 bending peaks at 1432 cm^{-1} are present in both untreated and alkali treated fiber. The increase in peak intensity at around ($1600\text{--}1650\text{ cm}^{-1}$) after alkaline treatment corresponds to the removal of wax, adhesives, pectin, and gummy substance from the fiber surface. The small peak at 1525 cm^{-1} is related to lignin component. This peak is not present in the alkali treated sample. It could be due to partial removal of lignin after alkali treatment. The peak at 1244 cm^{-1} is much smaller in alkali treated PALF than untreated sample. This peak corresponds to $\text{C}=\text{O}$ stretch of the acetyl group of lignin and is reduced because lignin is partially removed from the fiber surface.

Thermal Decomposition of Untreated and Treated Pineapple Leaf Fiber

TGA and DTG curves of untreated and alkali treated pineapple leaf fiber (2%, 4%, 6%, 8%, and 10 %) were shown in Fig. 2 and 3. Tests were performed from $25\text{ }^{\circ}\text{C}$ to $700\text{ }^{\circ}\text{C}$ in the nitrogen atmosphere at $10\text{ }^{\circ}\text{C}/\text{min}$ heating rate.

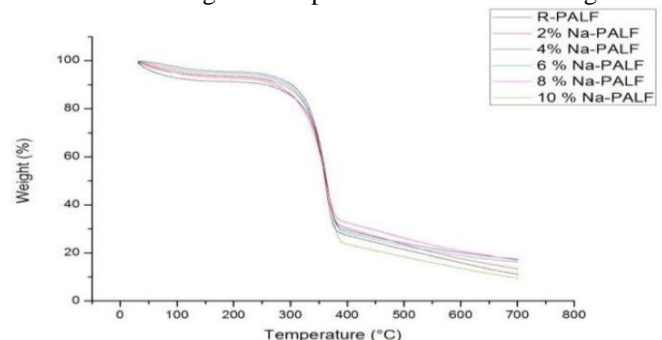


Fig. 2: TGA curve for untreated and alkali pineapple leaf fibers

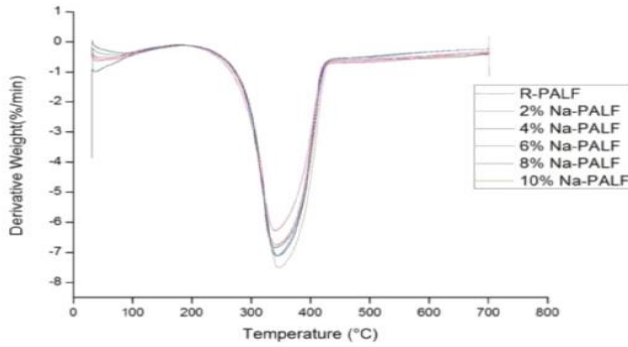


Fig. 3: DTG curve for untreated and alkali pineapple leaf fibers

The thermal decomposition of pineapple leaf fiber (untreated and alkali treated) was two-stage processes, where the first stage was the evaporation of water and extraction of volatile compounds and the second stage was the decomposition of hemicellulose, cellulose, and lignin component. Initial mass loss due to evaporation of water is common for all types of plant fiber but the rate of evaporation depends on the hydrophilicity of natural fiber [8]. The weight percentage of water extraction was reduced from 9% to 3% after 4 wt% NaOH treatment of PALF. This was because of the removal of a hydroxyl group and free water after alkaline treatment. Brigida *et al.* (2010) reported that structurally bound water is resistant to evaporation during drying [11]. Mortari Daniela A *et al.* (2014) found the mass loss of sugar cane bagasse around 8.7 wt% under the atmosphere of CO₂ [12]. As the natural fibers were heated, the weight of the material was reduced.

Thermal degradation data of untreated and treated PALF is tabulated in Table 3 where T_{onset} is the temperature at which degradation starts, $T_{d,1}$ & $T_{d,2}$ are the first and second stage of decomposition temperature and T_p is the peak temperature of maximum rate of degradation. Table 3 shows that the initial decomposition temperature of PALF was increased from 251.23 °C to 285.31 °C after 4 wt% NaOH treatment of fiber. This might be because of the removal of hemicellulose component. The presence of the carbonyl group (C=O) in hemicellulose may be responsible for lower thermal stability.

Table 3: Onset and degradation temperatures of raw pineapple leaf fiber obtaining from TGA thermogram

Sample	T_{onset} (°C)	$T_{d,1}$ (°C)	$T_{d,2}$ (°C)	T_p (°C)	Max. ROD ¹	R _m
R-PALF	251.23	360.6	526.09	341.58	6.85	10.89
2% Na-PALF	272.71	361.87	556.79	341.52	6.75	13.17
4% Na-PALF	285.31	363.37	603.97	343.43	7.13	17.24
6% Na-PALF	275.08	363.48	569.82	343.12	7.091	16.01
8% Na-PALF	263.36	362.07	619.18	339.72	6.28	16.83
10% Na-PALF	271.59	364.17	468.7	346.85	7.51	9.19

¹ROD: Rate of decomposition, R_m: Residual mass at 700°C

Stevulova Nadezda *et al.* (2016) reported that the primary decomposition of lignocellulosic materials occurs within 200-

400 °C [13]. Alwani M. Siti *et al.* (2014) found that sugarcane bagasse fiber had higher mass loss compared to coir fiber due to the presence of more hemicellulose content [6]. Table 3 also shows that initial decomposition temperature was reduced beyond 4% alkaline treatment. This was because of excess removal of hemicellulose. Ndazi Bwire S *et al.* (2007) reported the reduction in temperature of maximum weight loss by at least 26 °C, beyond 4 wt% alkaline treatment of rice husk fiber. This was due to the excess removal of cementing material like hemicellulose and lignin [14]. The second step of thermal degradation was ranging from 400-620 °C. It was observed that $T_{d,2}$ of untreated and alkali treated fiber at 526.09 °C, and 619.18 °C respectively, is from the decomposition of lignin. Panyasart Kloykamol *et al.* (2014) reported the first step decomposition temperature of alkaline (Na-PALF) treated and silane (Si-PALF) treated fiber higher than raw pineapple leaf fiber composite [10]. Table 4 reveals the percentage weight loss of untreated and treated PALF. It was observed that there is a delay in degradation temperature after alkaline temperature.

Table 4: Degradation temperatures (°C) for untreated and treated PALF

Wt. Loss (%)	R-PALF	2% Na-PALF	4% Na-PALF	6% Na-PALF	8% Na-PALF	10% Na-PALF
10	254.48	285.30	301.68	294.48	272.5	285.02
20	324.22	329.12	333.62	330.43	321.67	329.52
30	343.47	344.62	347.21	345.69	340.93	346.33
40	353.45	354.25	356.3	355.62	353.15	356.6
50	360.6	361.8	363.37	363.48	362.7	364.17

Na Lu *et al.* (2013) investigated the effect of alkaline treatment of 5 wt% at 50 °C on thermal decomposition of hemp fiber. They concluded that untreated hemp fiber degrade earlier than treated fiber [1]. Fig. 2 showed that the major mass loss (30-50%) occur at the temperature greater than 300 °C. This was because of the decomposition of cellulose and lignin. It was investigated that crystalline cellulose was degraded between the temperatures of 302-375 °C. The DTG curves show that at peak temperature, the rate of decomposition was increased from 6.83 %/min to 7.13 %/min due to 4% alkali treatment of pineapple leaf fiber. These results are because of depolymerization of native cellulose structure to short length crystallites.

Lignin was the most difficult component to decompose compared to other components because of its cross-linked highly complex aromatic structure of phenylpropane units. It starts to decompose at a lower temperature (typically 160-175 °C) compared to cellulose but it decomposed slowly under the whole temperature range and extend its temperature as high as 900 °C. The DTG curves for untreated and treated pineapple leaf fibers have reached the equilibrium stage beyond 400 °C where the rate of decomposition is approximately constant and lignin component of natural fiber decomposes slowly.

According to Paiva *et al.* (2006), the decomposition of lignin occurred in a wider temperature compared to cellulose and

hemicellulose [15]. After 700 °C, the remaining mass of pineapple leaf fiber was shown in Table 3. It was observed that the residue was increased up to 8% alkali treated fiber compared to the untreated one. This was due to the slow rate of the chemical decomposition reaction. Only ash and char was left after 700 °C. The differences in the amount of char left can be attributed to the change in chemical composition of pineapple leaf fiber after alkali treatment. It was reported by Williams (2004) that a high lignin content in natural fiber results in the production of a higher level of ash and char during pyrolysis [16]. The 10% NaOH treated PALF shows less residue content than untreated PALF. This might be due to excess delignification of pineapple fiber after 10% alkaline treatment.

4. LITERATURE REVIEW

There are many claims to the invention of the differential gear but it is likely that it was known, at least in some places, in ancient times. Some historical milestones of the differential include:

- Two Chinese Buddhist monks and engineers created South Pointing Chariots for Emperor Tenji of Japan. Documented Chinese reproductions of the South Pointing Chariot by Yan Su and then Wu Deren, which described in detail the mechanical functions and gear ratios of the device [5]
- Massimo guiggiani et al. (2006) studied, the dependency of steady-state cornering behaviour of vehicles on locked differential and investigation was done on the vehicle models having linear and nonlinear tyre behaviour, respectively [6].
- Daniel Chindamo et al. (2018) discussed the working principle and limitations of limited slip differential, used to enhance the traction capability [7].
- G. Mastinu et al. (1993) studied the limited-slip differential which is commonly used to enhance traction on slippery roads and helps high speed vehicles for a high speed turning at the bends [8].
- Athanassios Mihailidis et al. (2013) studied the evolution of differentials in automobiles and discussed the driving torque distribution as per requirement [9].
- C Doniselli et al. (2008) studied the limitations in mechanical differential system for traction control purpose and traction force distribution between the axles especially for front wheel drive vehicle [10]
- Chandrakant Singh et al. (2014) discussed the benefits of independent electric motor in electric vehicle driving and the way that it can replace the traditional mechanical differential gear system [11].
- Amit Suhane et al. (2017) studied the role of differential gear during adverse conditions like uneven, wet less traction roads etc [12].
- Modern automotive differential patented by watchmaker On Siphore Pecqueur in the period 1792-1852 of the Conservatoire des Arts Et M-tiers in France for use on a steam carts [13].

- Richard Roberts of England patented 'gear of Compensation', a differential for road locomotives in 1832[14].
- Aveling and Porter of Rochester, Kent list a crane locomotive in their catalogue fitted with their patent differential gear on the rear axle in the year 1874 [15].
- First use of differential on an Australian steam car by David Shearer was done in 1897[16].
- Packard introduces the spiral-gear differential, which cuts gear noise in the year 1913. Packard introduced the hypoid differential, which enable the propeller shaft and its hump in the interior of the car to be lowered in 1926[17].

5. DESIGNING OF AN OPEN DIFFERNETIAL

Gearing is one of the most critical components in a mechanical power transmission system, and in most industrial rotating machinery. It is possible that gears will predominate as the most effective means of transmitting power in future machines due to their high degree of reliability and compactness.

Every shaft has gears which are connected to each other by teeth. The two bodies have either rolling or sliding motion along the tangent at the point of contact. There are wide ranges of gears utilized by industry, yet every one of these gears has the same reason, which is to transmit motion starting from one shaft to other. Gear can be classified as Parallel shaft which are spur and helical gears, while the other one is intersecting shaft which are bevel and spiral gears.

Straight bevel gears are used in designing of the differential in the present study. The bevel gears are used for transmitting power at a constant velocity ratio between two shafts whose axes intersect at a certain angle. The pitch surfaces for the bevel gear are frustums of cones. The elements of the cones, intersect at the point of intersection of the axis of rotation, therefore the cones may roll together without sliding.

A. Gear failure

A pair of teeth in action is generally subjected to two types of stresses: bending and contact stresses [18]. Both these types of stresses may not attain their maximum values at the same point of contact. Due to the application of load on the gear teeth, the gear tooth is subjected to bending. When the same is repeated for a very huge number of cycles Bending Fatigue failure of the gear sets in. The fatigue in the gears induces the formation of cracks in the root of the gear tooth which propagates with each rotational cycle of the gear and ultimately leads to the failure of the gear tooth. Surface failure, like pitting or flaking due to contact stress may take place. Pitting is the formation of craters on the gear tooth surface. These craters are formed due to the high amount of compressive contact stresses in the gear surface occurring during transmission of the torque. Failure by bending will occur when the significant tooth stress equals or exceeds either the yield strength or the bending endurance strength. A surface failure occurs when the significant contact stress equals or exceeds the surface endurance strength. Hence the

bending stress and the contact stress should be always less than its maximum permissible value.

B. Methodology

1) CAD Model

A 3-D CAD model of the component gear pairs of the open differential was created using GearTrax software and was assembled using Solidworks. The gear tooth profile was taken as involute with pressure angle equal to 25°. The number of teeth for each gear was taken as follows:

Pinion bevel gear- 16

Ring bevel gear- 70

Differential side gear- 40

Differential pinion gear- 20

All the gears are straight bevel gears, and all mating gears are mounted on perpendicular and intersecting axes.

2) Conventional Design

Input parameters

Engine Torque = 90 Nm, 3500 rpm

Gearbox Ratio = 3.454:1

Final Drive Ratio = 4.375:1

Pressure angle (α) = 25°

3) Material selection

The material selection is based on the properties required by the gears. The materials should have high tensile strength, hardness and wear resistance. The material selected is AISI4340 Steel (40Ni18Cr4Mo2), a low alloy steel with 0.4 wt.% Carbon, 1.8wt.% Nickel, 0.4% Chromium and 0.2wt. % Molybdenum. This steel can be heat treated to have the combination of high hardness and toughness. The presence of Mo and Mn imparts high hardenability to the steel. This steel responds well to the surface hardening and tempering and recommended for automotive application in gears, valve rods, springs and shafts etc. The physical and Mechanical properties of the selected material are given in Table 1.

Table. 1: Material Properties Of 4340 Steel

Physical Properties	Metric
Density	7.85 gm/cc
Mechanical Properties	
Hardness, Brinell	321
Hardness, Knoop	348
Hardness, Rockwell B	99
Hardness, Rockwell C	35
Hardness, Vickers	339
Ultimate Tensile Strength	1110 MPa

Yield Strength	710 MPa
Elongation at break	13.2%
Reduction in area	36%
Modulus of elasticity	200 GPa
Poisson's ratio	0.29
Machinability	50%

AISI 4340 has a favourable response to heat treatment (usually oil quenching followed by tempering) and exhibits a good combination of ductility and strength when treated thusly. Uses include piston pins, bearings, ordnance, gears, dies, and pressure vessels.

This material was selected for the differential as it had adequate hardness and tensile strength. This ensured that the maximum bending stress and contact stress encountered by the gear tooth is well within the limiting stresses that this material could encounter without failure

Minimum number of teeth to avoid interference

To avoid interference the formative number of teeth on ring gear should be greater than

$$T' \geq \frac{2A_w}{G \left[1 + \frac{1}{G} \left(\frac{1}{G} + 2 \right) \sin^2 \phi - 1 \right]} \dots \dots \dots (1)$$

4) AGMA equation (Calculation of Bending and Contact Stress)

The American Gear Manufacturers Association (AGMA) [19] has for many years been the responsible authority for the dissemination of knowledge pertaining to the design and analysis of gearing. The methods this organization presents are in general use when strength and wear are primary considerations

The American Gear Manufacturers Association (AGMA) has established standards for the analysis and design of the various kinds of bevel gears

By using the equations given by AGMA (American Gears Manufactures Association) a more detailed analysis can be carried out as it takes in account several other factors

5) Lewis equation (Calculation of Bending stress)

Lewis equation considers only static loading and doesn't take the dynamics of meshing teeth into account. Lewis considered gear tooth as a cantilever beam with static normal force F applied at the tip. Assumptions made in the derivation are: 1. The full load is applied to the tip of a single tooth in static condition. 2. The radial component is negligible. 3. The load is distributed uniformly across the full-face width. 4. Forces due to tooth sliding friction are negligible. 5. Stress concentration in the tooth fillet is negligible. Lewis equation is given by

Lewis equation is given by:

$$\sigma = \frac{W_t}{F_p y} \dots \dots \dots (2)$$

W_t = tangential tooth load

p = diametral pitch

F = face width of tooth

σ = bending stress in gear tooth

$y = \text{Lewis form factor}$

Drawbacks of Lewis equation are:

- The tooth load in practice is not static. it is dynamic and is influenced by pitch line velocity.
- The whole load is carried by single tooth is not correct. Normally load is shared by teeth.
- The greatest force exerted at the tip of the tooth is not true as the load is sheared by teeth. It is exerted much below the tip when single pair contact occurs.
- The stress concentration effect at the fillet is not considered.

In mechanical engineering and tribology, Hertzian contact stress is a description of the stress within mating parts. This kind of stress may not be significant most of the time, but may cause serious problems if not take it into account in some cases

6) Hertz contact theory (Calculation of contact stress)

Hertz contact theory is derived from the analytical solution of elasticity theory equations [20].

- Surface are infinitely large half-spaces.
- Pressure profile is parabolic [20] (which assumes that the shape of the bodies in contact can also be approximated well with parabolic shapes, e.g., sphere, ellipse or a cylinder)
- All the assumptions of the classical theory of elasticity apply [21] (small strain, homogeneous material).

6. FINITE ELEMENT ANALYSIS (FEA)

Finite element analysis was done using ANSYS 14.5. It was done to find out the bending stress on a tooth of the drive pinion and the contact stress between teeth of the drive pinion and ring gear.

A. Bending stress

To determine the bending stress a force equal to the P_t (tangential component of the resultant force on the gear tooth) [22] is applied on the top of a tooth of the drive pinion. As the tooth is to be treated as a beam, the rest of the pinion except the tooth is fixed. Equivalent stress is then calculated using ANSYS 14.5. The resultant maximum bending stress is shown in Fig. 2

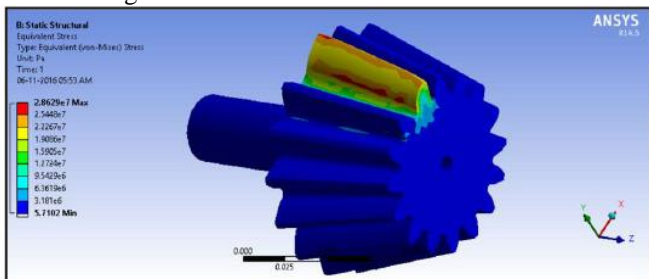


Fig. 2: Bending stress in gear tooth

B. Contact stress

To calculate the contact, stress a moment of 310.86 Nm is applied on the drive pinion, and frictionless supports are added to the pinion shaft and the ring gear bore. Equivalent

stress is calculated using ANSYS 14.5. which has been shown in Fig. 3

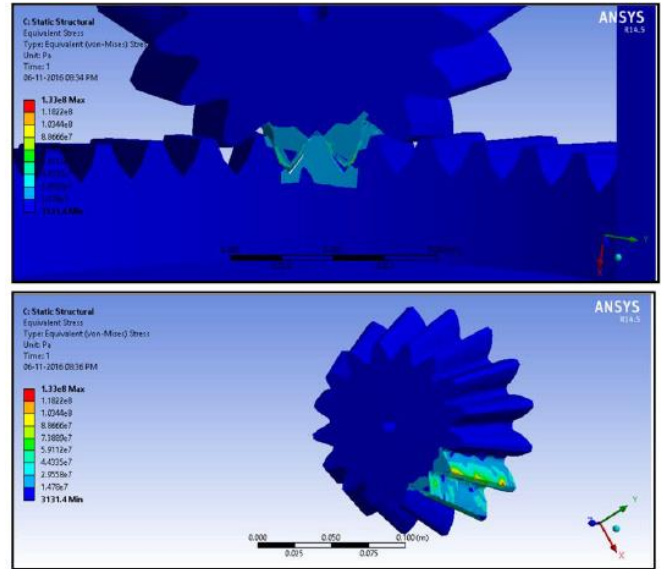


Fig. 3: Contact stresses in gear tooth

7. RESULT AND DISCUSSION

An open type differential is designed and analysed numerically and theoretically for a much-used saloon vehicle. The differential is designed to sustain highest stress conditions that it could encounter while the vehicle is plying. Straight bevel gears of different dimensions were used as constituents of the differential. The bending stress and contact stress encountered by the gear tooth of the differential pinion are calculated at highest torque conditions. Based on the design parameters, calculations are made by conventional modified Lewis and AGMA equations for bending stress. The contact stresses are computed using Hertz contact stress equation, AGMA prescribed equations. The results obtained from these analytical equations are compared with the results obtained from FEA analysis using ANSYS 14.5.

The results are as follows:

Table 2. Comparison Of The Maximum Bending Stress on Gear Teeth

	Lewis Equation	AGMA Equation	FEA
Maximum bending stress on gear teeth	32.5 MPa	23.38 MPa	28.63 MPa

Table 3. Comparison Of Maximum Contact Stress on Gear Teeth

	Hertz contact stress Equation	AGMA Equation	FEA
Maximum contact stress on gear teeth	346 MPa	707.5 MPa	133 MPa

The AGMA equation [23] introduce dynamic effects into consideration for better design. The Lewis criterion also takes the dynamic effects in to consideration but Hertz equations do not and hence give a higher magnitude of the stress.

Results of Contact stress obtained from FEA are more realistic as the modelling and boundary conditions are applied as per the real requirements and defies the assumption that only one tooth of a gear is in contact at a time and transmitting force and hence is calculated to be lower than that calculated by other methods. Although, analytical methods are much easier to understand by design engineers and provides the flexibility to get the predicted results instantly depending on design parameters and assumptions made.

The material chosen for the differential is AISI 4340. The maximum bending stress and maximum contact stress calculated are well under the limiting value. The factor of safety achieved is greater than 1 for both the stresses.

8. CONCLUSIONS

On the basis of comparison of results obtained from theoretical and numerical analysis of maximum bending stress and maximum contact stress on gear teeth using Lewis equation, AGMA and Hertz contact stress equation and using FEM software ABAQUS, presented in this paper in this paper, the following conclusions are drawn:

- The material chosen for the differential is AISI 4340. The maximum bending stress and maximum contact stress calculated are well under the limiting value. The factor of safety achieved is greater than 1 for both the criteria.
- The bending and contact stress of the differential gear teeth are calculated using Lewis, Hertz equations, AGMA equations and FEA. It is observed that Lewis criterion is highly conservative than AGMA and FEA.
- The stresses computed from analytical equations are found out to be within permissible limits and agrees well with the results obtained from FEA.

REFERENCES

- 1) H. Bayrakceken, "Failure analysis of an automobile differential pinion shaft," *Engineering Failure Analysis*, 13(8), 1422-1428, 2006.
- 2) (2018)[Online]. Available: <https://www.quora.com/Who-invented-the-differential-drive>
- 3) Amato, T., Frendo, F. and Guiggiani, M., 2004, Handling behaviour of vehicles with locked differential system.

- Paper presented at Fisita 2004, Barcelona, Spain, 23–27 May 2004.
- 4) (2018)[Online] Available: https://en.wikipedia.org/wiki/South-pointing_chariot
 - 5) F. Frendo, G. Greco, & M. Guiggiani, "Critical review of handling diagram and understeer gradient for vehicles with locked differential," *Vehicle System Dynamics*, 44(06), 431-447, 2006.
 - 6) M. Gadola, D. Chindamo, G. Legnani, & Comini, M., "Teaching automotive suspension design to engineering students: Bridging the gap between CAD and CAE tools through an integrated approach," *International Journal of Mechanical Engineering Education*, 0306419018762803, 2017.
 - 7) G. Mastinu, E. Battistini, "The influence of limited-slip differentials on the stability of rear-wheel-drive automobiles running on even road with dry surface," *International Journal of Vehicle Design*, 14(2-3), 166-183, 1993.
 - 8) A. Mihailidis, I. Nerantzis, "Recent Developments in Automotive Differential Design," In *Power Transmissions* pp. 125-140 Springer, Dordrecht, 2013.
 - 9) A. Doniselli, G. Mastinu, R. Cal, "Traction control for front wheel drive vehicle", *Vehicle System Dynamics*, pp. 87-104, 2008.
 - 10) A. Singh, L. Kumar, B. K. Dewangan, P. k. sen, S. K. Bohidar, "A Study on Vehicle Differential system," *International Journal of scientific research and management (IJSRM)*, 2014.
 - 11) A. Suhanea, R. S. Ranaa, R. Purohitb, "Prospects of Torsen Differential in Four Wheel Drive Automobile Transmission System," *Materials Today: Proceedings* 5 (2018) 4036–4045, 2017.
 - 12) (2018) Garfield Kart Tier list [Online] Available: <https://steamcommunity.com/sharedfiles/filedetails/?id=1462213589>
 - 13) J. M. Karande, N. S. Uttekar, V. P. Patil, S. A. Gawade, "Manufacturing of Simple Differential Locking System," *International Journal of Engineering Technology, Management and Applied Sciences*, 2015.
 - 14) AC08286419, A. (Ed.), *Vehicle system dynamics: international journal of vehicle mechanics and mobility*. Taylor & Francis, 1972.
 - 15) (2018)[Online] Available: <http://themicanic.weebly.com/uploads/4/3/5/7/4357357/differentials.pdf>
 - 16) V. B. Bhandari, *Design of Machine Elements*, 3rd Edition, McGraw Hill Publication, 2012.
 - 17) AGMA 908-B89, American Gear Manufacturers Association, 1500 King Street, Suite 201, Alexandria, Virginia 22314
 - 18) X. Zhu, Tutorial on Hertz Contact Stress. *Opti* 521, 1–8, 2012.
 - 19) G. M. Maitra, *Hand Book of Gear Design*, McGraw Hill Publication, 2004.
 - 20) R. BUDYNAS, J. Nisbett, *Shigley's Mechanical Engineering Design*, McGraw Hill Publication, 2008.